FULL PAPER

ADVANCED FUNCTIONAL MATERIALS

DOI: 10.1002/adfm.200700423

Soluble Phenanthrenyl-Imidazole-Presenting Regioregular Poly(3-octylthiophene) Copolymers Having Tunable Bandgaps for Solar Cell Applications**

By *Yao-Te Chang*, *So-Lin Hsu*, *Ming-Hsin Su*, and *Kung-Hwa Wei**

We have used Grignard metathesis polymerization to successfully synthesize a series of regioregular polythiophene copolymers that contain electron-withdrawing and conjugated phenanthrenyl-imidazole moieties as side chains. The introduction of the phenanthrenyl-imidazole moieties onto the side chains of the regioregular polythiophenes increased their conjugation lengths and thermal stabilities and altered their bandgap structures. The bandgap energies, determined from the onset of optical absorption, could be tuned from 1.89 eV to 1.77 eV by controlling the number of phenanthrenyl-imidazole moieties in the copolymers. Moreover, the observed quenching in the photoluminescence of these copolymers increases with the number of phenanthrenyl-imidazole moieties in the copolymers, owing to the fast deactivation of the excited state by the electron-transfer reaction. Both the lowered bandgap and fast charge transfer contribute to the much higher external quantum efficiency of the poly(3-octylthiophene)-side-chain-tethered phenanthrenyl-imidazole than that of pure poly(3-octylthiophene), leading to much higher short circuit current density. In particular, the short circuit current densities of the device containing the copolymer having 80 mol % phenanthrenyl-imidazole, **P82**, improved to 14.2 mA cm^{-2} from 8.7 mA cm^{-2} for the device of pure poly(3-octylthiophene), **P00**, an increase of 62 %. In addition, the maximum power conversion efficiency improves to 2.80 % for **P82** from 1.22 % for **P00** (pure **P3OT**). Therefore, these results indicate that our polymers are promising polymer photovoltaic materials.

1. Introduction

The development of conjugated polymers that possess extended delocalized π-electrons for use in organic optoelectronic devices has advanced dramatically in recent years. In particular, there have been extensive studies into solar cell devices based on bulk heterojunctions formed using conjugated polymers.[1–8] The structures of bulk heterojunction polymer solar cells have been prepared from a thin film of the electron-donating conjugated polymer and an electron-accepting species, which has been either another polymer or a set of nanoparticles. Polythiophene derivatives are recognized as being among the most promising materials for solar cell applications because of their excellent light absorption and electronic conductivity. Polymer solar cells containing blends of poly(3-hexylthiophene) and the buckminsterfullerene derivative [6,6]-phenyl-C_{61}-butyric acid methyl ester (PCBM) have been studied in depth; recent reports[3] have indicated that power conversion efficiencies of around 1 % ~2 % under standard solar conditions (AM 1.5G, 100 mW cm^{-2}, 25 °C). There are a number of ways to proceed toward improving the power conversion efficiencies of these polymer solar cells. For example, varying the annealing temperature and time—to lower the electrical resistance of the devices—and introducing a lower-work-function electrode have been reported.[9–13] Alternatively, copolymerization with different conjugated monomers has also been investigated, but with limited success in improving the power conversion efficiency.[10]

Semiconducting conjugated polymers that are used presently in light emitting diodes typically absorb in the range between 300 and 500 nm, which is only a small portion of the spectrum of sunlight. Thus, another approach toward higher-efficiency polymer solar cells is the use of conjugated polymers that absorb light more effectively. There are two main ways to tackle this problem. The first involves introducing chromophores that have different energy bandgaps into the conjugated polymers, thereby increasing the bandwidth of absorption. This method usually leads to some synthetic difficulties resulting from the typical bulkiness and low reactivity of functionalized chromophores or dyes. The second way is to incorporate electron-withdrawing moieties into side chains that are in conjugation with

[*] Prof. K. H. Wei, Y. T. Chang, S. L. Hsu, M. H. Su
Department of Materials Science and Engineering
National Chiao Tung University
1001 Ta Hsueh Road, Hsinchu, 30049 Taiwan (R.O.C.)
E-mail: khwei@mail.nctu.edu.tw

[**] We are grateful for the financial support provided by the National Science Council through Project NSC 95-2120M-009-007. We thank Hsu-Shen Wang for assisting in the synthetic aspects of this project. Supporting Information is available online from Wiley InterScience or from the authors.

ADVANCED FUNCTIONAL MATERIALS

the main polymer chains. In this way, not only the electron transfer efficiency of the excitons of the side-chain-tethered phenanthrenyl-imidazole polymers can be improved but also their bandgaps can be lowered for matching the wavelength of the maximum photon flux of sunlight (700 nm), which is ca. 1.77 eV.[14] The extent of the reduction in the bandgap of the side-chain-tethered phenanthrenyl-imidazole polymers will depend on the effective conjugation length of the system, which are sometimes reduced by steric hindrance. Previously, oxadiazo-, triazole-, quinoxaline-, imidazole-, and triazine-containing moieties are used in semiconducting polymers for other applications.[15] In this present study, we designed an extended conjugated molecular structure in which phenanthrenyl-imidazole moieties were attached covalently to the side chain of thiophene units to form regioregular copolymers that had lowered bandgaps—which were tunable depending on the content of phenanthrenyl-imidazole moieties—and enhanced electron transferring abilities. Because of the poor solubility of the phenanthrenyl-imidazole moiety, we used a thiophene monomer (3-octylthiophene) presenting a long alkyl chain to form copolymers exhibiting improved solubility. Scheme 1 displays our synthetic approaches toward the 2,5-dibromo-3-octylthiophene and the planar phenanthrenyl-imidazole moiety monomer. We expected that the presence of phenanthrenyl-imidazole moieties conjugated to the thiophene units would enhance the electron transfer of polythiophene and alter the energy levels of the highest occupied molecular orbitals (HOMOs) and lowest unoccupied molecular orbitals (LUMOs) of our polymers, thereby decreasing the bandgap and enhancing their photovoltaic properties. Scheme 2 displays the copolymerization of the 2,5-dibromo-3-octylthiophene **M1** and 2-(2,5-dibromothiophen-3-yl)-1-phenyl-1*H*-phenanthro[9,10-d]imidazole monomer **M2**, performed using a Grignard metathesis method.

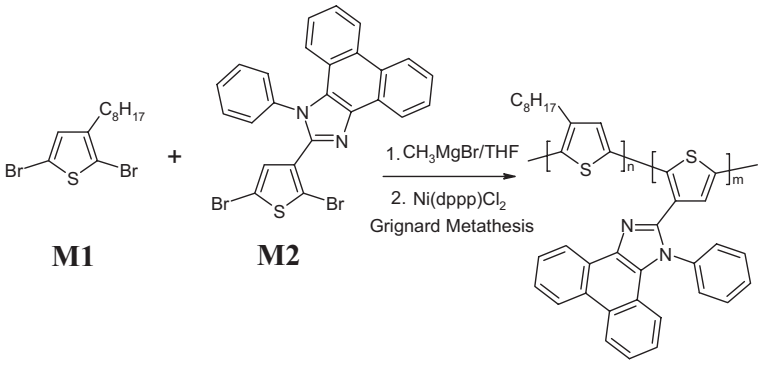

Polymer molar ratio	**P00**	**P55**	**P73**	**P82**
Molar fraction of **M1**	100%	50%	30%	20%
Molar fraction of **M2**	0	50%	70%	80%

Scheme 2. The Grignard metathesis polymerization of 2,5-dibromo-3-octylthiophene **M1** and 2-(2,5-dibromothiophen-3-yl)-1*H*-phenanthro[9,10d]imidazole **M2**; THF: tetrahydrofuran.

2. Results and Discussion

Figure 1 presents the ^{1}H NMR spectra of **M2** and some of the synthesized polymers. The regioregularity of the polymers can be determined from the ratio of the area under the peak at 6.98 ppm to the area under all of the peaks ranging from 6.98 to 7.04 ppm. Because only a signal at 6.98 ppm is present in the spectrum of **P00**, with no other peaks nearby, we believe that this polymer possesses an almost complete head-to-tail configuration (i.e., the regioregularity close to 100 %).[15] In the spectrum of **P37**, the peak at 6.73 ppm (CH proton of the thiophene ring) is absent, and the broad peaks in the ranges 8.2–9.2 (CH protons of the phenathrenyl group), 7.2–8.2 (CH protons on the phenyl group), and 0.8–3.0 ppm (octyl chain protons) confirm that the copolymers of **M1** and **M2** had formed.

Table 1 displays the molecular weight, the degradation temperature and the glass transition temperatures of synthesized copolymers, **P00** to **P82**. The number molecular weight (Mn) of our polymers range from 7.2 kg/mole to 11.6 kg/mole and the polydispersity index (PDI) shows at the range of 1.28 and 1.61. The thermal degradation temperatures of these copolymers increased upon increasing the content of phenanthrenyl-imidazole moieties. For instance, the degradation temperature of **P82** improved to 432.2 °C from 370.1 °C for **P00**, an increase of 62 °C. Whereas, the glass transition temperature of **P82** was not detectable as compared to 40 °C for **P00**.

Figure 2 displays UV-vis spectra of the polymers in the solid state. The small peak at 270 nm is caused by the presence of conjugated phenanthrenyl-imidazole moieties that are not fully coplanar to the polythiophene chain owing to steric hindrance. The π–π* transitions are responsible for the maximum absorp-

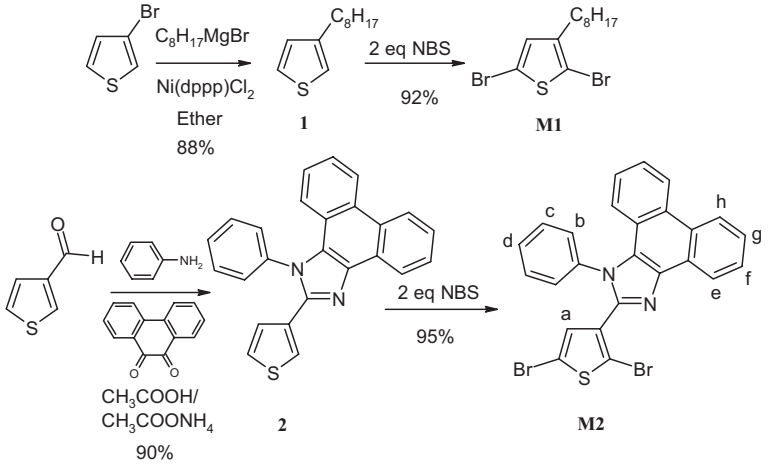

Scheme 1. The synthetic scheme of 2,5-dibromo-3-octylthiophene **M1** and **M2**; NBS: *N*-bromosuccinimide

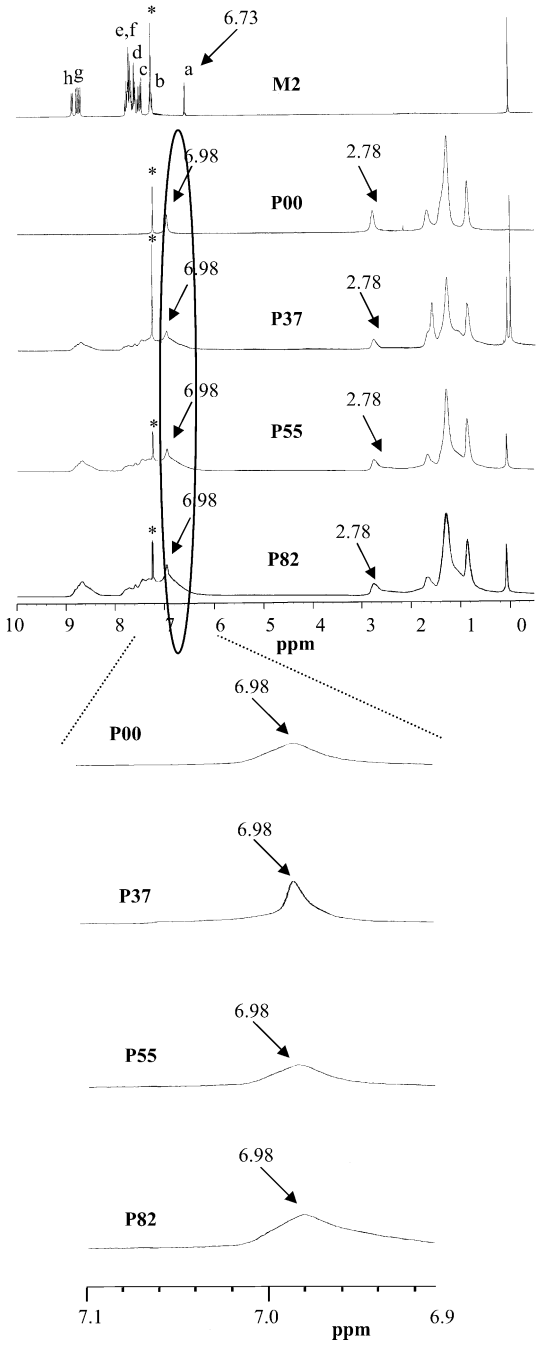

Figure 1. The ^{1}H NMR spectra of **M2**, **P00**, **P37**, **P55**, and **P82**.

tions (λ_{max}) that occur at ca. 520 nm for **P00** and 556 nm for **P82** thin films.[16] These data indicate that the optical bandgap of the **P82** copolymer is lower than that of pure **P3OT**. Table 2 lists the absorption maxima, and the optical bandgaps of the synthesized polymers. Optimally, conjugating 80 mol % of phenanthrenyl-imidazole moieties to the polythiophene chains led to the optical bandgap being reduced from 1.89 to 1.77 eV, confirming that the presence of the phenanthrenyl-imidazole moieties increases the effective conjugation length of the polythiophene main chain to some extent.[17] The cyclic voltammogram

Table 1. Molecular weights and thermal properties of the synthesized polymers.

	Mn[×10^3]	Mw[×10^3]	PDI	T_d[a] [°C]	T_g [°C]
P00	11.6	15.6	1.34	370.1	40.0
P55	11.2	17.8	1.61	404.5	[b]
P73	7.2	12.2	1.58	430.2	[b]
P82	7.7	9.9	1.28	432.2	[b]

[a] The temperature at which 5 % weight loss occurred based on the initial weight. [b] The glass transition temperature cannot be observed.

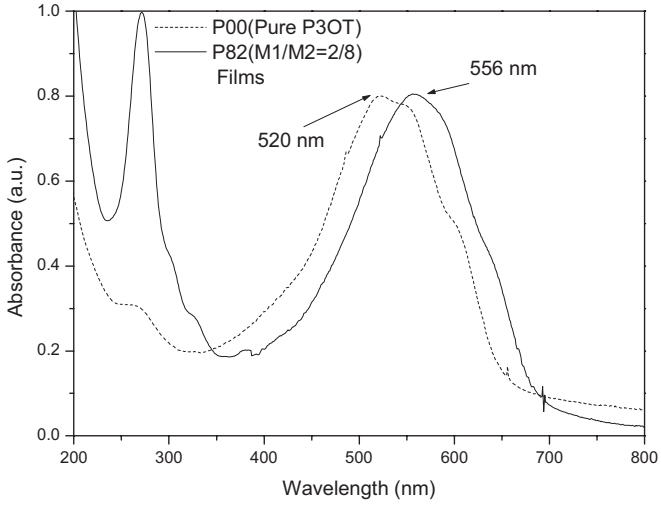

Figure 2. The UV-vis spectra of **P00** and **P82** recorded in the solid state.

Table 2. UV-Vis absorption peaks and optical bandgaps of synthesized polymers.

Polymer	Absorption	λ_{max}	Optical bandgap
	Solution [nm]	Film [nm]	[eV]
P00	439	520(549, 603)	1.89
P55	470	540(628)	1.82
P73	476	548(631)	1.81
P82	478	556(638)	1.77

data also shows the same trend, despite absolute values being different (see Supporting Information Table S1).

Figure 3 displays photoluminescence (PL) spectra of polymer films recorded at excitation wavelengths of 450 nm, respectively. The PL of the phenanthrenyl-imidazole-containing copolymers films was dramatically quenched relative to that of pure **P3OT**, with the degree of quenching increasing upon increasing the content of phenanthrenyl-imidazole units in the copolymer. This finding suggests that photoinduced charge transfer occurred from the photoexcited polythiophene backbone to the electron-withdrawing phenanthrenyl-imidazole side chains, and that this charge transfer was sufficiently rapid to compete with radiative recombination of the excitons.[18]

Figure 4 displays the photocurrents of diodes having the structure ITO/PEDOT:PSS/polymer: [6,6]-phenyl-C_{61}-butyric

ADVANCED FUNCTIONAL MATERIALS

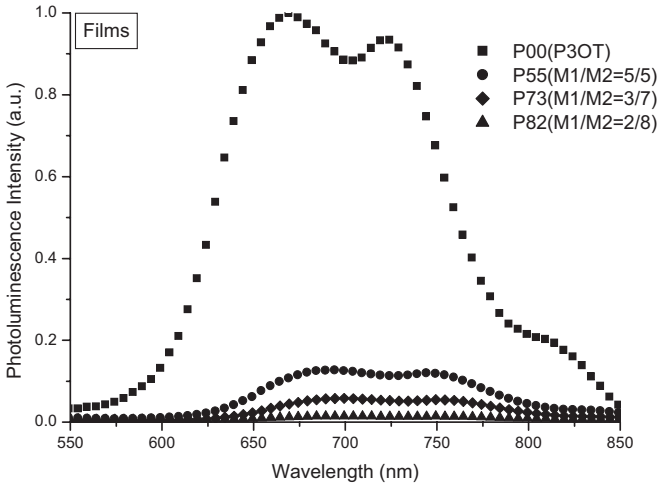

Figure 3. Photoluminescence (PL) spectra, normalized to the number of absorbed photons, of synthesized polymers in the solid state.

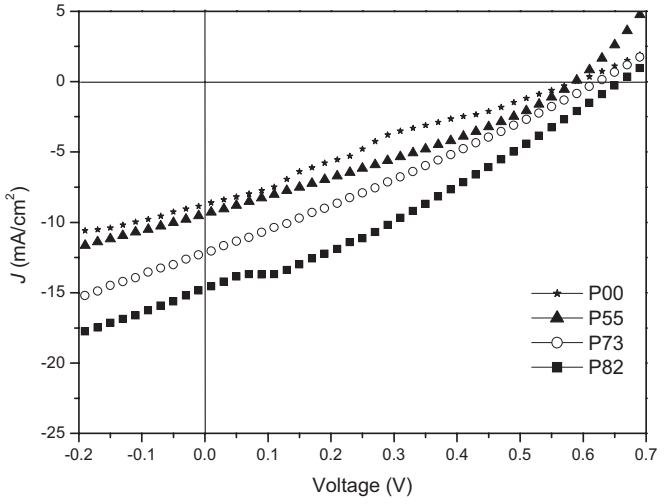

Figure 4. Current density-voltage characteristics of illuminated (AM 1.5G, 100 mW cm^{-2}) polymer solar cells incorporating **P00**, **P55**, **P73**, and **P82** and PCBM.

acid methyl ester (PCBM) (1:2, w/w)/Ca/Al that were illuminated at AM 1.5 G and 100 mW cm^{-2}. In Figure 4, the short circuit current density (J_{sc}) increased upon increasing the content of the phenanthrenyl-imidazole moieties, probably as a consequence of enhanced light absorption at longer wavelength due to the extended conjugation and the fast charge transfer of the copolymers.[19] For all efficiency values reported in this paper we used a spectral mismatch factor of 0.8 to account for deviations in the spectral output of the solar simulator with respect to the standard AM 1.5 spectrum and deviations in the spectral response of the device with respect to that of the reference cell. Table 3 lists the detailed photovoltaic properties of these polymer solar cells. In particular, the short circuit current densities of the device containing the copolymer having 80 mol % phenanthrenyl-imidazole, **P82**, improved to 14.2 mA cm^{-2} from 8.7 mA cm^{-2} for the device of pure poly(3-octylthiophene), **P00**, an increase of 62 %. Because of the increased degree of the short circuit current density that occurred when the phenanthrenyl-imidazole content increased, the current density-voltage characteristics of our solar cell devices suggest that charge transfer occurred from the photoexcited polythiophene backbone through the phenanthrenyl-imidazole moieties and PCBM to the electrode. The open circuit voltages (V_{oc}) of the **P82** heterojunction device increased to 0.69 V from 0.59 V for the **P00** device. The open circuit voltages of polymer heterojunction cell is usually proportional to the difference between the lowest unoccupied molecular orbital (LUMO) of the electron acceptor and the highest occupied molecular orbital (HOMO) of the electron donor[20] but are influenced by many other factors, for example, solvent effects.[21] In the **P82** device case, it appears that the fact that the copolymers became less soluble and less miscible with PCBM at higher phenanthrenyl-imidazole moieties contents[21] dominates over the decrease between the LUMO of the electron acceptor and the HOMO of the electron donor, resulting in a slightly higher V_{oc} than that of the **P00** device. Nevertheless, the filled factors remained low as a result of the devices maintaining large series resistances and low shunt resistances.[22] Even with the disadvantage of low filled factors, the power conversion efficiency increased dramatically to 2.8 % for **P82** from 1.22 % for **P00**, presumably due to the lowered bandgap and the enhanced electron transfer for the former polymer. The photophysics of the devices using the synthesized copolymers can be manifested by examining their external quantum efficiency and light absorption data. Figure 5a and b show the external quantum efficiency (EQE) of the polythiophene side-chain-tethered phenanthrenyl-imidazole/PCBM devices and the UV-vis absorption of the copolymer/PCBM blends experienced the same annealing condition as that of the device, respectively. The EQE values of **P82** device is at least 19 % larger than that of the **P00** device at wavelength from 400 to 600 nm. In a detailed comparison, the EQE value of the **P82** device improved to 50 % from 29 % for the **P00** device at 450 nm incident light, almost 100 % increase. The maximum EQE value of the **P82** and **P00** devices reaches 69 % and 29 %, respectively, at 480 nm, with a 1.5 times increase. Even at a much longer wavelength of 600 nm, the EQE of **P82** device improved to 33 % from 11 % for **P00** device, a two-fold increase. The relative light absorption intensity of **P82**/PCBM blend is about 20 % higher than that of **P00**/PCBM

Table 3. Photovoltaic properties of the polymer solar cells.

Weight ratio of polymer to PCBM	V_{oc} [V]	J_{sc} [mA/cm^2]	FF [%]	PCE [%]
P00:PCBM = 1:2	0.59	8.7	23.6	1.22
P55:PCBM = 1:2	0.64	9.4	30.2	1.68
P73:PCBM = 1:2	0.62	12.4	28.0	2.15
P82:PCBM = 1:2	0.69	14.2	31.1	2.80

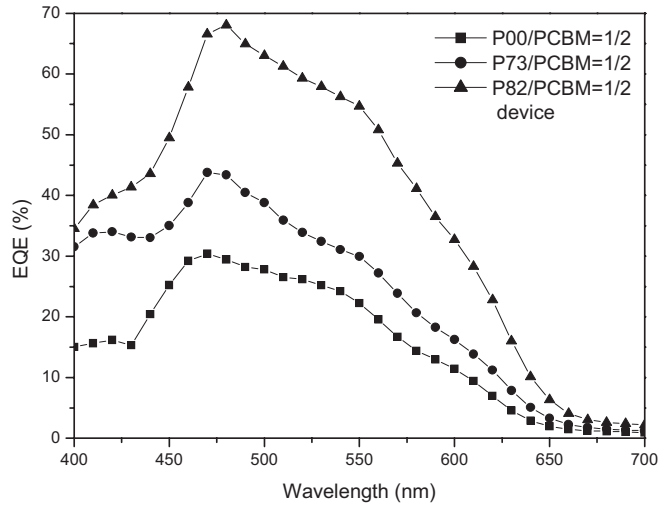

(a)

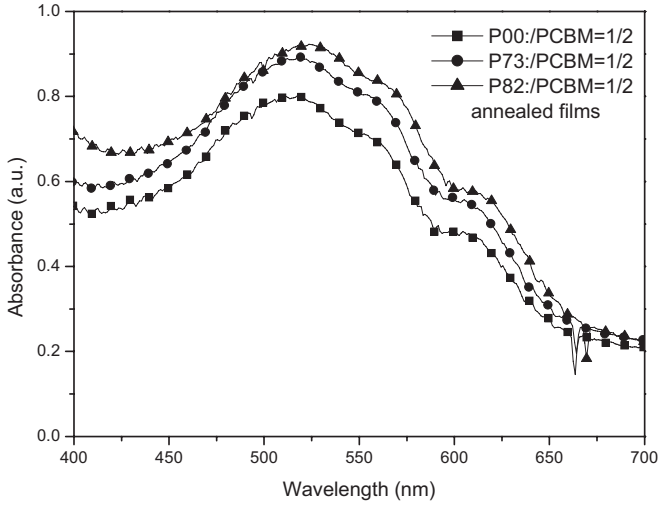

(b)

Figure 5. a) The external quantum efficiency of **P00**, **P73** and **P82**/PCBM solar cells. b) The UV-vis absorption of the copolymer/PCBM blends experience the same annealing condition as that of the device.

blend at 400 nm and 600 nm, respectively. The similarity between the shape of the EQE curves of these copolymers and their corresponding UV-vis absorption spectra indicated that the enhanced photocurrent current densities, J_{sc}, are mainly generated by the rapid electron transfer of the dissociated excitons in polythiophene backbone to the conjugated phenanthrenyl-imidazole side chain and lowered bandgap of the copolymers. The large increase in the short-circuit current density of the polythiophene-side-chain tethered phenanthrenyl-imidazole device in turn accounts for the large increase in the power conversion efficiency of **P82** device as compared to that of **P00** device. These results demonstrate that the introduction of electron-withdrawing and conjugated phenanthrenyl-imidazole onto polythiophene side chains can quite effectively improve the photon conversion efficiency of poly(3-octylthiophene).

3. Conclusions

We have prepared a new family of regioregular thiophene copolymers presenting phenanthrenyl-imidazole side chains in conjugation with the main polymeric chain, leading to lowered bandgaps. The reduction in the bandgap energy in conjunction with the observed photoluminecsence quenching indicates that rapid charge transfer occurred from the photoexcited polythiophene backbone through the phenanthrenyl-imidazole moieties to PCBM in the device. The much higher external quantum efficiency of the polythiophene-side-chain-tethered phenanthrenyl-imidazole device than that of pure poly(3-octylthiophene) device results in much higher short circuit current density. Due to the high short circuit current density obtained in the phenanthrenyl-imidazole presenting regioregular poly(3-octylthiophene), the power conversion efficiency improved dramatically to 2.80 % for the copolymer containing 80 mol % phenanthrenyl-imidazole from 1.22 % for pure poly(3-octylthiophene).

4. Experimental

Materials: Chemicals were purchased from Aldrich, TCI, or Lancaster. [6,6]-phenyl-C_{61}-butyric acid methyl ester (PCBM) was perchased from Nano-C. Polyethylenedioxythiophene/polystyrenesulphonate (PEDOT/PSS) was perchased from Baytron (P VP A1 4083).

Preparation of Monomers: Scheme 1 illustrates the synthetic route used for the preparation of the monomers 2,5-dibromo-3-octylthiophene (**M1**) and 2-(2,5-dibromothiophen-3-yl)-1-phenyl-1*H*-phenanthro[9,10-d]imidazole (**M2**).

1-Phenyl-2-(3-thienyl)-1*H*-phenanthro[9,10-d]imidazole (**2**), which was prepared from the reaction of 3-thiophenecarboxaldehyde, phenanthrenequinone, aniline, ammonium acetate, and acetic acid, was isolated in 92 % yield. The structure of compound **2** was verified using ^{1}H and ^{13}C NMR spectroscopy and mass spectrometry. **M2** was prepared from the reaction of compound **2** with NBS; it was isolated in 93 % yield [23]. Detailed synthetic procedures and characterization data are provided in the Supporting Information.

Preparation of Polythiophene Derivatives: All polymers were synthesized through Grignard metathesis polymerizations in THF, according to procedures similar to those described in the literature [15b,15c]. The Grignard metathesis polymerizations of 2,5-dibromo-3-octylthiophene (**M1**) and 2-(2,5-dibromothiophen-3-yl)-1-phenyl-1H-phenanthro[9,10-d]imidazole (**M2**) are illustrated in Scheme 2. Detailed synthetic procedures and characterization data are provided in the Supporting Information.

^{1}H and ^{13}C NMR spectra were recorded on a Varian Unity-300 NMR spectrometer. Infrared spectra were recorded from KBr disks on a Nicolet Protégé-460 FTIR spectrophotometer. Elemental analyses (EA) of our polymers were performed using a Heraeus CHN-OS Rapid instrument. Thermal gravimetric analyses of the polythiophene derivatives were performed using a Du Pont TGA 2950 instrument operated at a heating rate of 10 °C min^{-1} under a nitrogen purge. Differential scanning calorimetry (DSC) was performed on a Du Pont DSC 2010 instrument operated at a heating rate of 10 °C min^{-1} under a nitrogen purge. Samples were heated from 30 to 200 °C, cooled to 20 °C, and then heated again from 30 to 200 °C; the glass transition temperatures (T_g) were determined from the second heating scans. The redox behavior of each polymer was investigated through cyclic voltammetry using an electrolyte of 0.1 M tetrabutylammonium hexafluorophosphate (n-Bu_4NPF_6) in acetonitrile. Cyclic voltammetry was performed using a BAS 100 electrochemical analyzer operated at a potential scan rate of 40 mV s^{-1}. In each case, a glassy disk carbon elec-

ADVANCED FUNCTIONAL MATERIALS

trode coated with a thin layer of the polymer was used as the working electrode. A platinum wire was used as the counter electrode and a silver wire was used as the quasi-reference electrode. All of the potentials quoted herein are referenced to the Ag wire as the quasi-reference electrode; the electrochemical potential of Ag is –0.02 V versus SCE. $E_{HOMO} = -E_{ox} - 4.4$ eV and $E_{LUMO} = -E_{red} - 4.4$ eV, where E_{ox} and E_{red} are the onset potentials of the oxidation and reduction peaks (versus saturated calomel electrode, SCE), respectively, and the value of 4.4 eV relates the SCE reference to a vacuum [16a]. UV-vis spectra were measured using an HP 8453 diode array spectrophotometer. PL spectra were recorded using a Hitachi F-4500 luminescence spectrometer. The molecular weights of the polythiophene derivatives were measured through gel permeation chromatography (GPC) using a Waters chromatography unit interfaced to a Waters 2414 differential refractometer. Three 5-μm Waters styragel columns were connected in series in decreasing order of pore size (10^4, 10^3, and 10^2 Å); THF was the eluent and standard polystyrene samples were used for calibration.

Device Fabrication: The current density-voltage (*J–V*) measurements of our polymers were performed using devices having a sandwich structure (ITO/PEDOT:PSS/polymer:PCBM (1:2, w/w)/Ca/Al). An ITO-coated glass substrate was pre-cleaned and treated with oxygen plasma prior to use. The polymer/PCBM layer was spin-coated at 1500 rpm from the corresponding dichlorobenzene solution (15 mg mL^{-1}). The nominal thickness of the polymer/PCBM layer was ca. 80 nm. Using a base pressure below 1×10^{-6} Torr, a layer of Ca (30 nm) was vacuum-deposited as the cathode and then a thick layer of Al (100 nm) was deposited as the protecting layer and the effective area of one cell is 0.04 cm^2. Testing of the devices was performed under simulated AM1.5 irradiation (100 mW cm^{-2}) using a xenon lamp-based Newport 66902 150W solar simulator. A Xenon lamp with AM1.5 filter was used as the white light source, and the optical power at the sample was 100 mW cm^{-2} detected by OPHIR thermopie 71964. The *J–V* characteristics were measured using a Keithley 236 electrometer. The spectrum of our solar simulator had a mismatch of less than 25 %. Reported efficiencies are the averages obtained from four devices prepared on each substrate. The external quantum efficiency (EQE) was measured using a Keithley 236 coupled with Oriel Cornerstone 130 monochromator. The light intensity at each wavelength was calibrated with OPHIR 71580 (diode).

Received: April 13, 2007
Revised: May 24, 2007
Published online: September 20, 2007

[1] a) C. Ego, D. Marsitzky, S. Becker, J. Zhang, A. C. Grimsdale, K. Müllen, J. D. MacKenzie, C. Silva, R. H. Friend, *J. Am. Chem. Soc.* **2003**, *125*, 437. b) J. Pei, W. Yu, J. Ni, Y. Lai, W. Huang, A. J. Heeger, *Macromolecules* **2001**, *34*, 7241.

[2] J. H. A. Smits, S. C. J. Meskers, R. A. J. Janssen, A. W. Marsman, D. M. D. Leeuw, *Adv. Mater.* **2005**, *17*, 1169.

[3] a) J. Liu, E. N. Kadnikova, Y. Liu, M. D. McGehee, J. M. J. Fréchet, *J. Am. Chem. Soc.* **2004**, *126*, 9486. b) J. Liu, T. Tanaka, K. Sivula, A. P. Alivisatos, J. M. J. Fréchet, *J. Am. Chem. Soc.* **2004**, *126*, 6550. c) A. M. Ramos, M. T. Rispens, J. K. J. V. Duren, J. C. Hummelen, R. A. J. Janssen, *J. Am. Chem. Soc.* **2001**, *123*, 6714. d) P. Schilinsky, U. Asawapirom, U. Scherf, M. Biele, C. J. Brabec, *Chem. Mater.* **2005**, *17*, 2175.

[4] G. Yu, J. Gao, J. C. Hummelen, F. Wudl, A. J. Heeger, *Science* **1995**, *270*, 1789.

[5] W. U. Huynh, J. J. Dittmer, A. P. Alivisatos, *Science* **2002**, *295*, 2425.

[6] K. M. Coakley, M. D. McGehee, *Chem. Mater.* **2004**, *16*, 4533.

[7] T. J. Savenije, J. E. Kroeze, X. Yang, J. Loos, *Adv. Funct. Mater.* **2005**, *15*, 1260.

[8] Y. Liu, M. A. Summers, C. Edder, J. M. J. Fréchet, M. D. McGehee, *Adv. Mater.* **2005**, *17*, 2960.

[9] V. D. Mihaiketchi, H. Xie, B. D. Boer, L. J. A. Koster, P. W. M. Blom, *Adv. Funct. Mater.* **2006**, *16*, 699.

[10] J. Hou, Z. Tan, Y. Yan, Y. He, C. Yang, Y. F. Li, *J. Am. Chem. Soc.* **2006**, *128*, 4911.

[11] K. Sivula, Z. T. Ball, N. Watanabe, J. M. J. Fréchet, *Adv. Mater.* **2006**, *18*, 206.

[12] G. Li, V. Shortriya, J. Huang, Y. Yao, T. Moriarty, K. Emery, Y. Yang, *Nat. Mater.* **2005**, *4*, 864.

[13] T. Erb, U. Zhokhavets, G. Gobsch, S. Raleva, B. Stühn, P. Schilinsky, C. Waldauf, C. J. Brabec, *Adv. Funct. Mater.* **2005**, *15*, 1193.

[14] K. M. Coakley, M. D. McGehee, *Chem. Mater.* **2004**, *16*, 4533.

[15] a) R. D. McCullough, R. D. Lowe, M. Jayaraman, D. L. Anderson, *J. Org. Chem.* **1993**, *58*, 904. b) M. C. Iovu, E. E. Sheina, R. R. Gil, R. D. McCullough, *Macromolecules* **2005**, *38*, 8649. c) E. E. Sheina, S. M. Khersonsky, E. G. Jones, R. D. McCullough, *Chem. Mater.* **2005**, *17*, 3317.

[16] A. R. Murphy, J. Liu, C. Luscombe, D. Kavulak, J. M. J. Fréchet, R. J. Kline, M. D. McGehee, *Chem. Mater.* **2005**, *17*, 4892.

[17] J. Roncali, *Chem. Rev.* **1997**, *97*, 173.

[18] F. Giacalone, J. L. Segura, N. Martin, M. Catellani, S. Luzzati, N. Lupsac, *Org. Lett.* **2003**, *5*, 1669.

[19] C. Waldauf, P. Schilinsky, J. Hauch, C. J. Brabec, *Thin Solid Films* **2004**, *451–452*, 503.

[20] M. C. Scharber, D. Mühlbacher, M. Kopper, P. Denk, C. Waldauf, A. J. Heeger, C. J. Brabec, *Adv. Mater.* **2006**, *18*, 789.

[21] J. Liu, Y. Shi, Y. Yang, *Adv. Funct. Mater.* **2001**, *11*, 420.

[22] W. Ma, C. Yang, X. Gong, K. Lee, A. J. Heeger, *Adv. Funct. Mater.* **2005**, *15*, 1617.

[23] S. Hotta, S. D. D. V. Rughooputh, A. J. Heeger, *Synth. Met.* **1987**, *22*, 79.